Discharge Characteristics of Cross-Shaped Microdischarge Cells in ac-Plasma Display Panel

Bo-Sung Kim, Ki-Duck Cho, Heung-Sik Tae, *Member, IEEE*, Sang-Hun Jang, and Young-Mo Kim

***Abstract*—This paper proposes a highly efficient cross-shaped cell structure to improve the luminous efficiency of an alternate current plasma display panel (ac-PDP). The microdischarge characteristics of the proposed structure are examined in an all-green 6-in test panel with various pressures and Xe-concentrations. Since the proposed cross-shaped cell structure has a longer Indium Tin Oxide (ITO) path between the two sustain electrodes and wider sidewall phosphor area, the following microdischarge characteristics were observed when compared with the conventional stripe-type cell structure. First, the sustain voltage margin was lower by about 15 V under a high Xe-concentration of 10%. Second, the rate of increase in the luminous efficiency was higher with a high pressure and high Xe-concentration. Finally, when adopting an auxiliary address pulse driving scheme, the luminous efficiency was improved by about 44% (2.38 lm/W) with a high Xe-concentration of 10%.**

***Index Terms*—Alternate current plasma display panel (ac PDP), cross-shaped cell structure, delta pixel, high luminous efficiency, high Xe-concentration, long Indium Tin Oxide (ITO) path, wide phosphor area.**

I. Introduction

DESPITE their predominant position in the flat-panel large-screen (>40 in) digital television market, plasma display panels (PDPs) still have a low luminous efficiency. Various attempts have been made to solve this problem, including optimizing the gas chemistry with a high Xe-concentration and the development of a new driving scheme and cell structure. In particular, the cell structure, i.e., barrier rib structure, is an important factor for improving the luminous efficiency, as the discharge volume and phosphor surface area strongly depend on the shape of the barrier rib. Thus, highly efficient cell structures, such as delta pixel structures, have recently been suggested to improve the luminous efficiency of an ac-PDP [1]–[3]. Such delta pixel structures can reduce the nondischarge area, while simultaneously extending the discharge area, thereby producing a high luminous efficiency due to the maximal use of the discharge area and enlarged open area for visible emission. However, the discharge characteristics under a high Xe-concentration [4] and sufficient driving margin conditions still need to be studied further.

Manuscript received August 21, 2004; revised January 28, 2005. This work was supported in part by the Regional Research Center Program of the Ministry of Commerce, Industry and Energy of Korea and in part by the Brain Korea 21 Project.

B.-S. Kim, K.-D. Cho, and H.-S. Tae are with School of Electronic and Electrical Engineering, Kyungpook National University, Daegu 702-701, Korea (e-mail: hstae@ee.knu.ac.kr).

S.-H. Jang and Y.-M. Kim are with the Materials Laboratory, Samsung Advanced Institute of Technology, Suwon, Kyunggi-Province 440-600, Korea.

Digital Object Identifier 10.1109/TPS.2005.848621

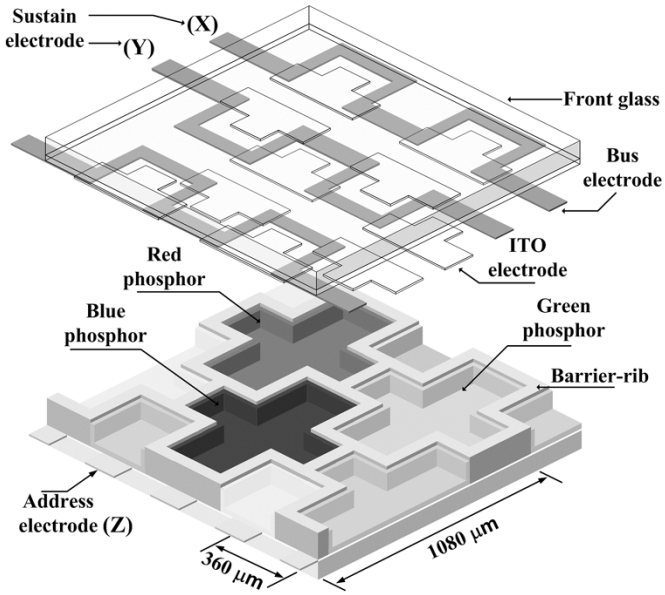

Fig. 1. Schematic diagram of single pixel for cross-shaped cell structure.

Accordingly, this paper proposes a highly efficient cross-shaped cell structure with a delta pixel color array to improve the luminous efficiency of an ac-PDP. The discharge characteristics of the cross-shaped cell structure are examined under a high Xe-concentration of 10% and various pressures, including an auxiliary address pulse-driving scheme [5]–[7]. In addition, to investigate the microdischarge characteristics relative to the auxiliary address pulse, an image-intensified charge-coupled device (ICCD) camera is used to measure the images of the infrared (IR: 828 nm) emitted from the cross-shaped cells.

II. Experiment

A. Experimental Setup

Fig. 1 shows a schematic diagram of a single pixel in the cross-shaped cell structure used in the current study. The vertical and horizontal cell pitches for a single pixel are 1080 and 360 μm, respectively. As shown in Fig. 1, the bus electrodes are placed on top of the barrier-ribs to enlarge the open area for visible emission, while patterned T-shaped Indium Tin Oxide (ITO) [8] sustain electrodes are arranged along the cell structure.

Figs. 2(a) and (b) show the detailed dimensions of a single cell for both the proposed cross-shaped barrier rib and the conventional stripe-type barrier rib. The specifications of the proposed cross-shaped cell employed in this research are compared with those of the conventional cell in Table I, where the ITO path of

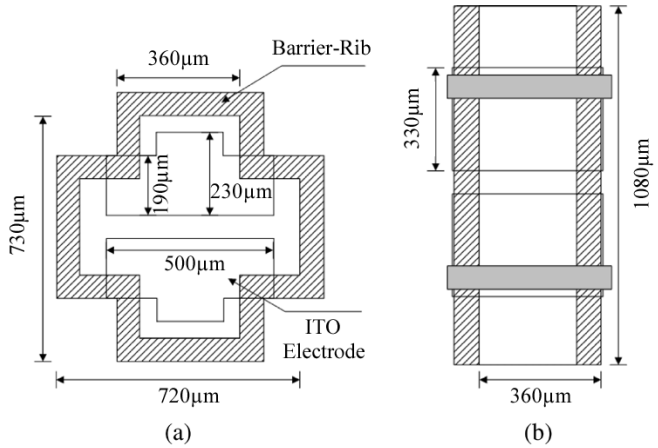

Fig. 2. Detailed dimensions of single cell for both (a) cross-shaped and (b) conventional stripe-type barrier ribs.

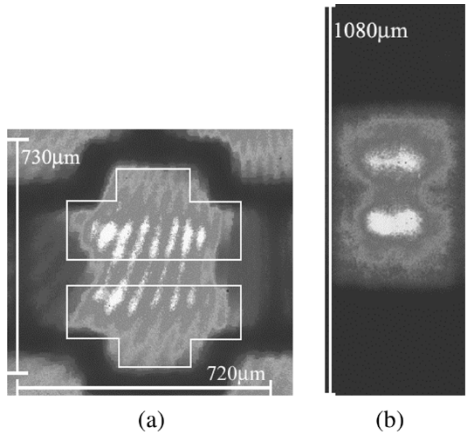

Fig. 3. Comparison of IR emission images for (a) cross-shaped and (b) conventional stripe-type cells measured by ICCD camera.

TABLE I
COMPARISON OF SPECIFICATIONS BETWEEN PROPOSED CROSS-SHAPED CELL AND CONVENTIONAL STRIPE-TYPE CELL

	Cross-shaped Cell	Conventional Stripe-type Cell
ITO Width	-	310 μm
ITO Gap	70 μm	70 μm
ITO Path (1cell)	500 μm	290 μm
Bus Electrode Width	80 μm	80 μm
Address Electrode Width	150 μm	150 μm
Barrier-rib Width	80 μm	80 μm
Barrier-rib Height	120 μm	120 μm
Cell Pitch	1080 X 360 μm	1080 X 360 μm

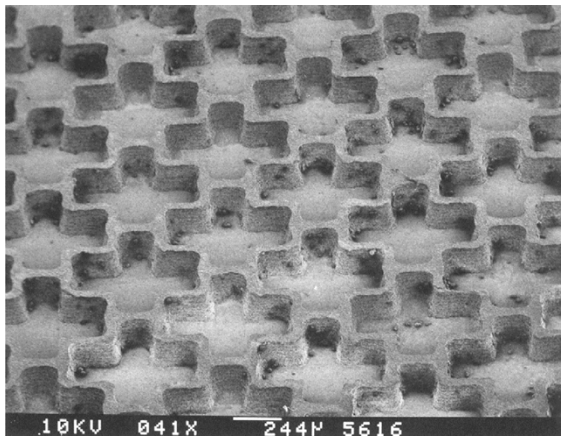

Fig. 4. SEM image of cross-shaped barrier-ribs fabricated by sandblasting method.

the cross-shaped cell is longer than that of the conventional cell. The area of the patterned T-shaped sustain electrode in the proposed cross-shaped cell structure is almost the same as that of the sustain electrode in the conventional striped cell structure. Here, the ITO path is defined as the length of the ITO electrode faced each other. As shown in Fig. 2, the ITO path is 500 μm for the cross-shaped cell, whereas the ITO path is 290 μm for the conventional cell. The cross-shaped barrier rib structure has 12 sidewalls, giving it a 21% larger sidewall phosphor area and 9% larger total phosphor area than the conventional stripe-type cell (hereinafter, the conventional cell). Furthermore, the effecttive discharge area of the cross-shaped cell structure is increased by eliminating the nondischarge area in the conventional cell.

Fig. 3 shows the IR emission images measured from both (a) the cross-shaped cell and (b) the conventional stripe-type cell by using the ICCD camera. As shown in Fig. 3, due to the long ITO path of the patterned T-shaped sustain electrode, the cross-shaped cell increased the phosphor area participating in the discharge (hereinafter, "effective phosphor area") considerably. From the IR emission data by the ICCD camera, it was observed that the effective phosphor area of the cross-shaped cell was increased by about 40% when compared with that of the conventional cell. This increase in the effective phosphor area in the cross-shaped cell structure is expected to contribute the increase in the visible conversion capability of the phosphor area. Fig. 4 shows a scanning electron microscope (SEM) image of the cross-shaped barrier ribs of the test panel fabricated using a sandblasting method. An MgO protective layer with a thickness 0.5 μm was then deposited on the dielectric layer with a thickness of 30 μm.

B. Measurement System

The measurement system consisted of a 6-in test panel, driving circuit system, current meter, color analyzer (CA-100), oscilloscope, and ICCD camera. Conventional cell structures were fabricated in the upper half of the 6-in test panel, while the proposed cross-shaped cell structures were fabricated in the lower half. A gas mixture of Ne–Xe (4%, 7%, and 10%) was used under various pressures, such as 300, 400, 500, and 600 torr, in the 6-in test panel. In particular, when adopting the driving waveform in Case 2 in part C, the changes in the IR emission relative to the auxiliary address pulse were measured using the ICCD camera, where an optical filter with a center wavelength of 828 nm and full width half maximum (FWHM) of approximately 10 nm were used to measure the IR (828 nm) emission images emitted from the top view of the test panel with a cross-shaped cell structure. To measure the time-averaged IR emission images and temporal behavior of the IR emission images, the shutter mode and gate mode of the

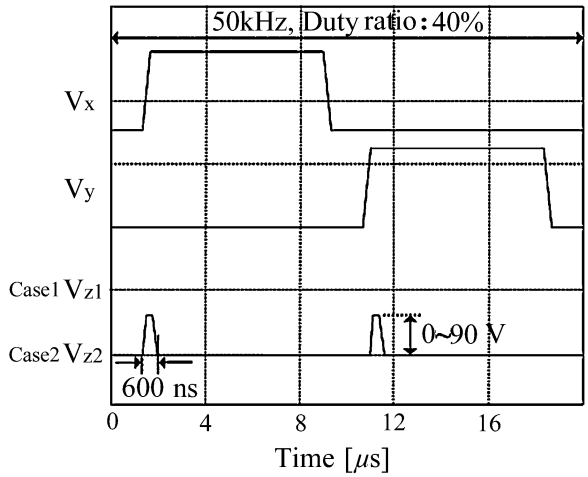

Fig. 5. Two driving waveforms applied during sustain-period in current study. (a) Case 1, where no address pulse is applied to address electrode. (b) Case 2, where address pulse is applied to address electrode.

ICCD camera were used, respectively, where the shutter mode meant that the IR emission was superposed during an exposure time of 10 ms, while the gate mode meant that the IR emission was superposed during an exposure time of 20 ns, thereby providing information on the time behavior of the IR emission from the test cell relative to a variation in the auxiliary address pulse. Only the green phosphor layers were deposited. The green phosphor used in this experiment was Zn_2SiO_4:Mn2+. The 282 × 21 pixels of the test panel were used to measure the luminance and the power consumption.

C. Driving Waveforms

Fig. 5 shows the two driving waveforms applied during a sustain period in the current study. In Case 1, only the sustain pulses V_x and V_y were applied to the sustain electrodes X and Y and no pulse was applied to the address electrode Z. Meanwhile, in Case 2, the auxiliary address short pulse V_z was synchronously applied to the address electrode Z along with the application of the sustain pulses V_x and V_y. It has been previously reported that the synchronous application of an auxiliary address short pulse can help improve the luminous efficiency [5], [6]. As such, the driving waveform in Case 2 was used to check the dependence of the auxiliary address short pulse effect [5], [6] on the shape of the barrier rib structure. The amplitudes of the sustain pulses V_x and V_y applied to the two sustain electrodes X and Y were 170 V for the cross-shaped cell, and 180 V for the conventional cell. The voltage difference of about 10 V between the two cell structures was due to the different sustain voltage margin, as shown in Table II. In addition, the same amplitude (= 180 V) of the sustain pulses V_x and V_y were applied to the two sustain electrodes X and Y to compare the discharge characteristics of both the conventional cell and the cross-shaped cell structures. For the auxiliary address short pulse in Case 2, the amplitudes were varied at intervals of 10 V from 0 to 90 V, however, the width was fixed at 600 ns. For the sustain pulses V_x and V_y the duty ratio was 40% and the operation frequency 50 kHz. For the Cases 1 and 2, the rising and falling times of the sustain pulse were 200 ns, whereas the rising and falling times of the auxiliary address short pulse were 100 ns, respectively.

TABLE II
COMPARISON OF FIRING AND SUSTAIN VOLTAGES BETWEEN PROPOSED CROSS-SHAPED CELL AND CONVENTIONAL STRIPE-TYPE CELL

	Cross-shaped Cell	Conventional Stripe-type Cell
First On	252 V	257 V
First Off	163 V	179 V

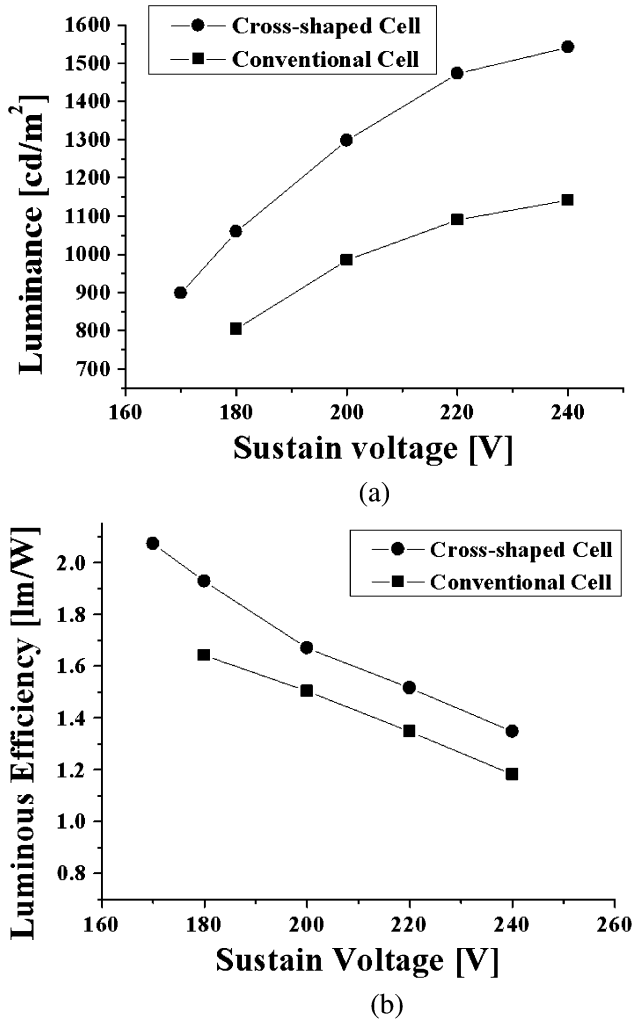

Fig. 6. (a) Luminance and (b) luminous efficiency characteristics of proposed cross-shaped and conventional cells relative to sustain voltage at Xe-concentration of 10% and pressure of 450 torr.

III. RESULTS AND DISCUSSION

Figs. 6(a) and (b) show the luminance and luminous efficiency characteristics of the proposed cross-shaped and conventional cells relative to the sustain voltage at a Xe-concentration of 10% and pressure of 450 torr, respectively. The green phosphors of both structures were the same, but, as shown in Fig. 6(a), the saturation characteristics of the luminance for the green phosphor layers showed a little different tendency for both types. For the conventional cell structure, the luminance was saturated at the sustain voltage of about 210 V, whereas for the cross-shaped cell structure, the luminance was not saturated until the sustain voltage of 230 V. This is also due to the difference of the phosphor areas participating in the discharge, i.e., the effective phosphor areas between both structures.

TABLE III
CHANGES IN LUMINOUS EFFICIENCY RELATIVE TO PRESSURE AND Xe-CONCENTRATION AT NEAR MINIMUM SUSTAIN VOLTAGE FOR BOTH CROSS-SHAPED AND CONVENTIONAL CELLS

	Xe 4 %		Xe 7 %		Xe 10 %	
	Luminous Efficiency		Luminous Efficiency		Luminous Efficiency	
	ConV.	Cross	ConV.	Cross	ConV.	Cross
300 Torr	1.165	1.236	1.27	1.382	1.363	1.517
400 Torr	1.294	1.426	1.398	1.564	1.512	1.732
500 Torr	1.408	1.565	1.536	1.78		1.972
600 Torr	1.488	1.786	1.659	1.947		2.189

TABLE IV
CHANGES IN LUMINOUS EFFICIENCY RELATIVE TO Xe-CONCENTRATION AT VARIOUS SUSTAIN VOLTAGE UNDER CONSTANT PRESSURE OF 450 TORR

	4 %		7 %		10 %	
	Luminous Efficiency		Luminous Efficiency		Luminous Efficiency	
	ConV.	Cross	ConV.	Cross	ConV.	Cross
150 V	1.611	1.875				
160 V	1.502	1.741	1.689	2.064		
180 V	1.322	1.432	1.469	.679	1.575	1.861
200 V	1.104	1.244	1.21	1.404	1.311	1.587
220 V			1.026	1.2	1.117	1.455
240 V			0.915	1.058	0.983	1.277
260 V					0.877	1.121

The proposed cross-shaped cell exhibited a higher luminance and luminous efficiency than the conventional cell, possibly due to its increased effective phosphor area, which enabled the visible conversion rate of the phosphor to increase with an increase in the intensity of the vacuum ultraviolet (VUV). Furthermore, the minimum sustain voltage for the cross-shaped cell was observed to be lower by about 15 V than that for the conventional cell under a high Xe-concentration of 10%, meaning that the cross-shaped cell had a lower sustain voltage margin than the conventional cell. This lower minimum sustain voltage (ΔV_{smin} = about 15 V) may be another factor for improving the luminous efficiency in the cross-shaped cell structure, which means that the sustain discharge can be produced by the weaker electric field in the Case of the cross-shaped cell. The reason for the lower minimum sustain voltage was not clear, but this low minimum sustain voltage was presumably due to the patterned T-shaped electrode, which meant that the facing ITO path was long and most of the ITO electrode was apart from the barrier rib of the cross-shaped cell.

However, in both cell structures, the changes in the luminance and luminous efficiency characteristics relative to the sustain voltage showed a typical tendency, i.e., the luminance increased in proportion to the increase in the sustain voltage, whereas the luminous efficiency decreased.

Table III shows the change in the luminous efficiency relative to the pressure and Xe-concentrations at a near minimum sustain voltage for both the cross-shaped cell and the conventional cell. The sustain voltage was 170 V for the cross-shaped cell and 180 V for the conventional cell. As shown in Table III, the luminous efficiency tended to increase with an increase in pressure, irrespective of the cell structure and various Xe-concentrations. However, the results in Table III also show that the rate of increase in luminous efficiency with an increase in pressure strongly depended on the cell structure. In the Case of a low Xe-concentration of 4%, when the pressure was increased from 300 to 600 torr, the luminous efficiency improved from 1.23 lm/W for the cross-shaped cell and 1.16 lm/W for conventional cell to 1.78 lm/W for the cross-shaped cell and 1.48 lm/W for conventional cell. As such, the rate of increase in the luminous efficiency, ΔL, when increasing the pressure was greater with the cross-shaped cell than with the conventional cell, i.e., for Xe concentrations of 4% and 7%, $\Delta L = 0.55$ and 0.56 lm/W for the cross-shaped cell and $\Delta L = 0.32$ and 0.38 lm/W for the conventional cell, respectively. The difference in the rate of increase in the luminous efficiency between the two structures was due to the difference in the effective phosphor area. It is well known that the VUV emission intensity increases in proportion to an increase in the gas pressure. However, the emission of phosphor shows saturation characteristics in the Case of an increase in the intensity of the VUV. Accordingly, if the phosphor area, namely the effective phosphor area increases, the visible conversion rate of the phosphor will also increase with an increase in the intensity of the VUV. This means that increasing the effective phosphor area is very important, especially under a high Xe-concentration. As shown in the cross-shaped cell structure in Table III, with a high Xe-concentration of 10%, the rate of increase in the luminous efficiency, ΔL, when increasing the pressure from 300 to 600 torr showed a maximum value of about 0.67 lm/W.

Table IV shows the changes in the luminous efficiency relative to the Xe-concentration at various sustain voltages under a constant pressure of 450 torr. As the sustain voltage increased, the corresponding luminous efficiency decreased for both the cross-shaped and conventional cells. In the case of a sustain voltage of 180 V, when the Xe concentration was increased from 4% to 10%, the luminous efficiency improved from 1.43 lm/W for the cross-shaped cell and 1.32 lm/W for the conventional cell to 1.86 lm/W for the cross-shaped cell and 1.57 lm/W for the conventional cell. The rate of increase in the luminous efficiency, ΔL, when increasing the Xe concentration from 4 to 10% was greater for the cross-shaped cell than for the conventional cell, i.e., for sustain voltages of 180 and 200 V, $\Delta L = 0.43$ and 0.34 lm/W for the cross-shaped cell and $\Delta L = 0.25$ and 0.21 lm/W for the conventional cell, respectively. As mentioned in Table III, the difference in the rate of increase in the luminous efficiency between the two structures was seemingly due to the difference in the effective phosphor area.

The proper application of the auxiliary positive address short pulse to the address electrode can promote the additional excitation or ionization due to the acceleration of the electrons toward the address electrode, which results in decreasing the discharge current toward the sustain electrode and simultaneously increasing the discharge current toward the address electrode.

Figs. 7(a) and (b) show the changes in the sustain discharge current and address discharge current as a function of the auxiliary address voltage pulse in the case of applying (a) the different sustain voltages and (b) the same sustain voltage, respectively. When varying the auxiliary address pulse, the sustain and

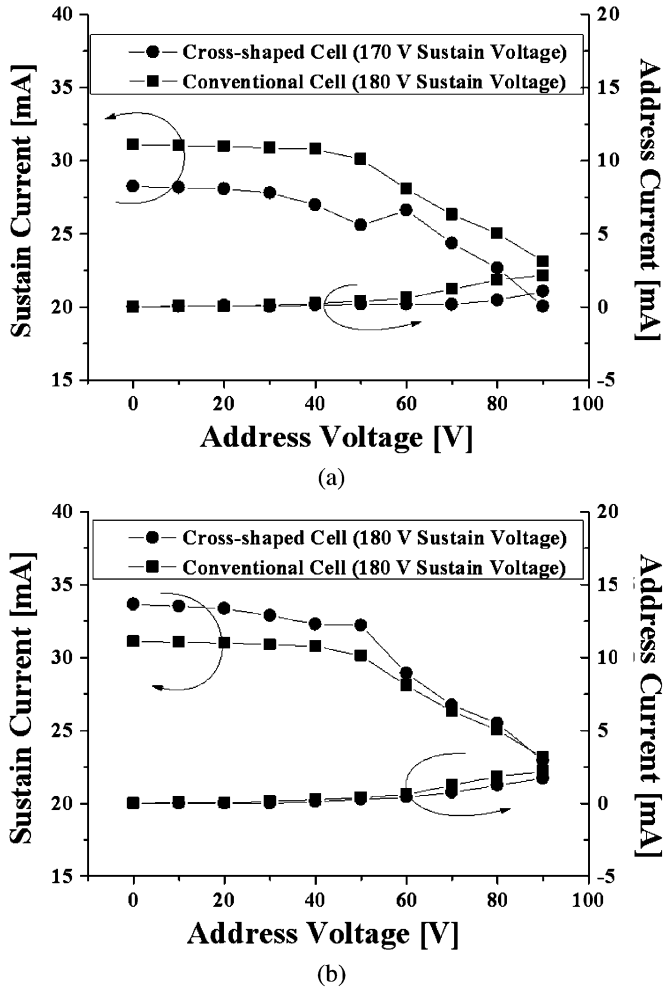

Fig. 7. Changes in sustain discharge current and address discharge current as function of auxiliary address voltage pulses where sustain voltages are (a) 170 V for cross-shaped cell and 180 V for conventional cell and (b) 180 V for both cross-shaped and conventional cells.

address currents exhibited the same tendency, irrespective of the type of cell structure: only when the auxiliary address pulse greater than 50 V was applied, the sustain current decreased considerably, while the address current increased slightly. As shown in Fig. 7(b), when the same sustain voltage was applied, the sustain current of the cross-shaped cell was higher than that of the conventional cell, but the address currents were almost the same for both the cell structures. The higher sustain current for the cross-shaped cell structure is due to the long ITO path of the T-shaped electrode. As the auxiliary address voltage increased, the difference of the sustain current between the two types of the cell structures decreased, as shown in Fig. 7(b). However, the sustain voltage can be lowered in the cross-shaped cell structure. In the case of adopting the low sustain voltage in the cross-shaped cell (170 V for the cross-shaped cell, and 180 V for the conventional cell), the sustain current of the cross-shaped cell is lower than that of the conventional cell, as shown in Fig. 7(a), but the luminance of the cross-shaped cell is higher than that of the conventional cell, as shown in Fig. 6(a). Therefore, the increase in the effective phosphor area plus the low sustain voltage results in a high luminous efficiency in the cross-shaped cell structure.

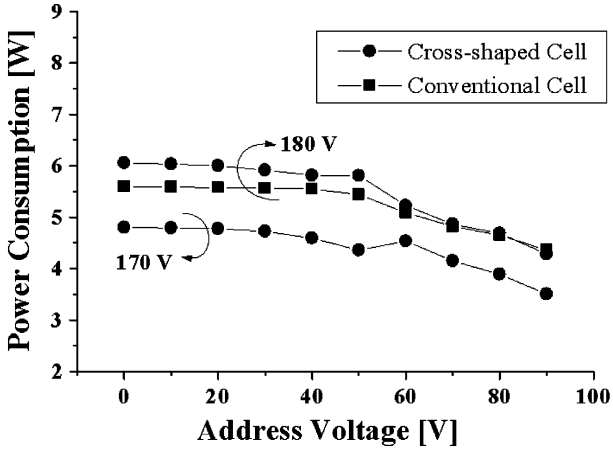

Fig. 8. Changes in power consumption as function of auxiliary address voltage pulses.

Fig. 8 shows the power consumptions for both the cross-shaped cell and conventional cell structures with the auxiliary address voltage at two different sustain voltages: 170 and 180 V, respectively. In general, the power consumption was slightly reduced with T-shaped electrode since its electrode area was reduced. In this experiment, the area of the patterned T-shaped sustain electrode in the proposed cross-shaped cell structure was almost the same as that of the sustain electrode in the conventional striped cell structure. When the same sustain voltage was applied, the power consumption of the cross-shaped cell was higher than that of the conventional cell structure at the auxiliary address voltage less than 60 V, whereas the power consumption of the cross-shaped cell was almost the same as that of the conventional cell structure at the auxiliary address voltage greater than 60 V.

Fig. 9 shows the changes in the luminous efficiency when varying the amplitude of the auxiliary pulse with a constant width of 600 ns. The luminous efficiency was obtained from the following equation:

$$\eta = \frac{\pi BA}{P} = \frac{\pi BA}{V_S(I_{\rm on} - I_{\rm off}) + V_A(I_{\rm on} - I_{\rm off})}$$

where η is a luminous efficiency, B is a luminance, A is a display area, and P is the power consumption considering both the sustain current and address currents. In the above equation, V_s is input sustain voltage, V_A is input auxiliary address voltage, $I_{\rm on}$ is discharge current, and $I_{\rm off}$ is displacement current.

As shown in Fig. 9, in the case of applying an auxiliary pulse greater than 40 V, the luminous efficiency was improved for both the cross-shaped cell and the conventional cell. At the same sustain voltage of 180 V, the maximum luminous efficiencies were obtained at the auxiliary pulse voltage of 60 V for both the structures. However, at the sustain voltage of 170 V for the cross-shaped cell, the luminous efficiency was increased with an increase in the auxiliary pulse voltage greater than 60 V. With an increase in the amplitude of the auxiliary address pulse greater than 40 V, the rate of increase in the luminous efficiency was found to be higher with the cross-shaped cell than with the conventional cell, as shown in Fig. 9, which was also seemingly due to the difference in the effective phosphor area between the two cell structures.

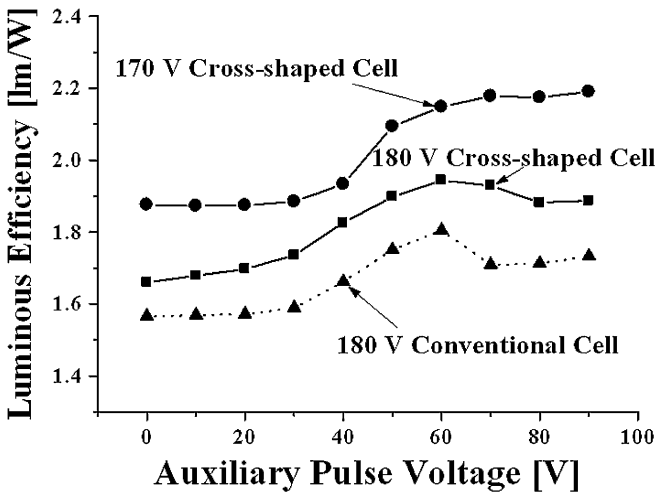

Fig. 9. Changes in luminous efficiency with variation in amplitude of auxiliary pulse at constant pulse width of 600 ns.

The measurement data of the IR emission for both the structures in Fig. 10(a) show that the IR emission for the cross-shaped cell is slightly increased, but, as shown in Fig. 6(a), the luminance for the cross-shaped cell structure is much increased at the same sustain voltage. This result means that the improvement of the luminous efficiency for the cross-shaped cell seems to be mainly due to the increase in the visible conversion capability by the phosphor layer instead of the increase in the discharge efficacy itself. Fig. 10(b) also shows the change in the IR emission in the Case of applying the auxiliary pulse for the cross-shaped cell. As shown in Fig. 10(b), the application of the auxiliary pulse for the cross-shaped cell causes a fast discharge and an intensification in the IR emission.

Fig. 11 shows time-averaged IR emission images measured from the top view of the cross-shaped cell structure using the shutter mode of the ICCD camera when the amplitude of the address pulse was varied at intervals of 10 V from 0 to 90 V at a constant pulse width of 600 ns. The Xe-concentration was 10% and the sustain voltage was 170 V. As shown in Fig. 11, when the auxiliary address pulse was less than 40 V, there was hardly any change in the behavior of the IR emission in the cross-shaped cell. However, when the auxiliary address pulse was higher than 50 V, the IR emission intensity was intensified and its area shrank along the address electrode in proportion to the amplitude of the auxiliary address pulse.

Fig. 12(a) shows the temporal behavior of the IR emission measured from the top view of the cross-shaped cell structure using the gate mode of the ICCD camera when varying the amplitude of the auxiliary address pulse with a constant pulse width of 600 ns. The Xe-concentration was 10% and the sustain voltage was 170 V. Fig. 12(b) shows the corresponding sustain and auxiliary address voltages at the specific discharge time shown in the IR emission images of Fig. 12(a). Since the rising time of the sustain voltage was 200 ns, the sustain voltage was 140 V at the time of 180 ns in Fig. 3(a) and remained 170 V during the discharge from 200 to 600 ns in Fig. 3(a). On the other hand, since the rising time of the auxiliary address voltage was 100 ns, the auxiliary address voltage continued to be the applied voltage during the discharge from 180 to

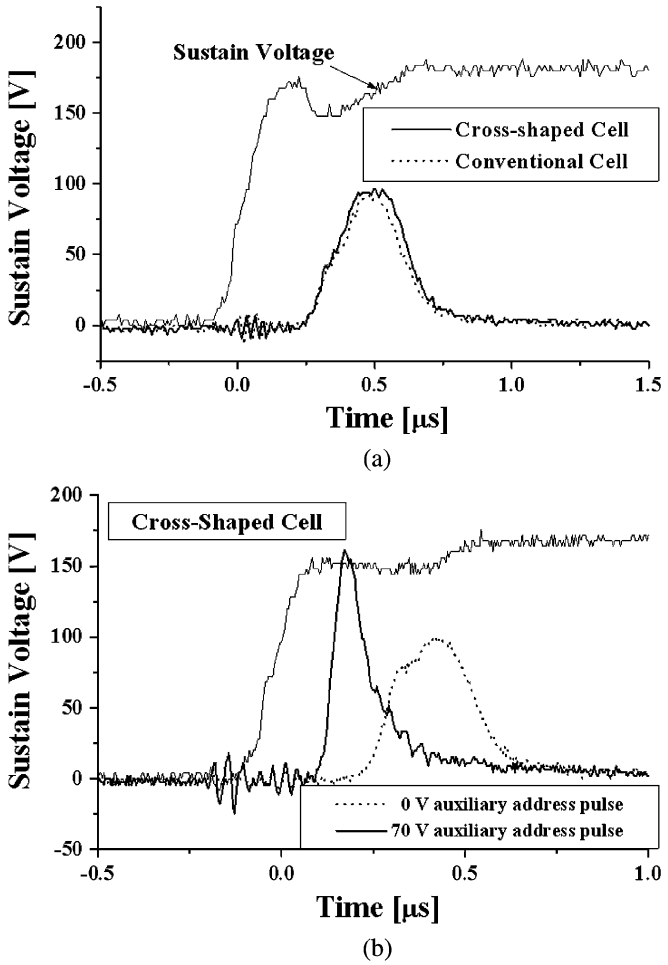

Fig. 10. (a) Comparison of IR intensities for cross-shaped and conventional cells at sustain voltage of 180 V (b) IR intensities for cross-shaped cell employing auxiliary address pulse.

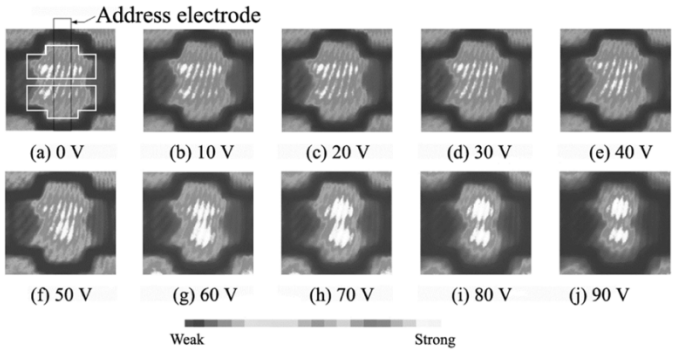

Fig. 11. Time-averaged IR emission images measured from top view of cross-shaped cell structure using shutter mode of ICCD camera when varying amplitude of address pulse at intervals of 10 V from 0 to 90 V at constant pulse width of 600 ns. (a) 0 V. (b) 10 V. (c) 20 V. (d) 30 V. (e) 40 V. (f) 50 V. (g) 60 V. (h) 70 V. (i) 80 V. (j) 90 V.

600 ns in Fig. 3(a). In a single cell in Fig. 12(a), the upper part of the ITO electrode is a cathode electrode, while the lower part of the ITO electrode is an anode electrode. [The detailed configuration of the ITO electrodes within a single cell is marked in the last cell in (ii) of Fig. 12(a).] As shown in (i) of Fig. 12(a), when no auxiliary pulse was applied, the discharge was initiated at about 320 ns at the center edge of

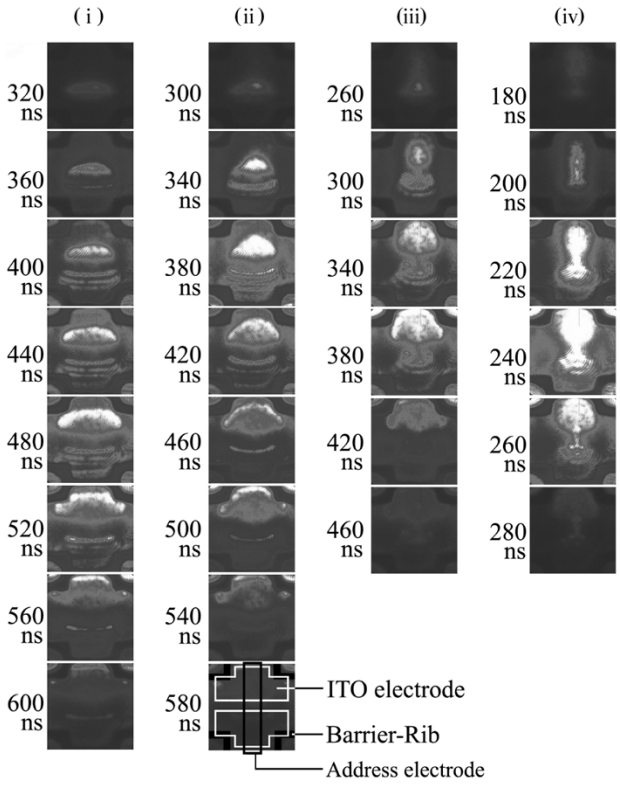

Fig. 12. Temporal behavior of IR emission images measured from top view of cross-shaped cells using gate mode of ICCD camera when varying amplitude of auxiliary address pulse at constant pulse width of 600 ns. (i) $V_z = 0$ V (ii) $V_z = 0$ V (iii) $V_z = 60$ V (iv) $V_z = 80$ V.

the anode electrode, then spread toward the cathode electrode. The maximal intensity of the discharge was at 480 ns and it was terminated at about 600 ns. The formation of striations was also observed at the anode electrode. With an auxiliary address pulse of 40 V, even though the discharge initiation seemed to be slightly faster, the temporal behavior of the discharge was essentially unchanged when compared to that with an auxiliary address pulse of 0 V. However, when applying an auxiliary address pulse of 60 and 80 V, fast discharge initiations were made at 260 and 180 ns, respectively, at the center of the anode electrode, which then spread toward the cathode electrode, plus fast terminations were made at 460 and 280 ns, respectively. As shown in the IR image at 380 and 240 ns in (iii) and (iv) of Fig. 12(a), respectively, the discharges were more spread out over the cathode electrodes along the address electrodes, due to the application of the auxiliary address pulse to the address electrode. Thus, the ICCD observation confirmed that the enlarged discharge area resulting from the application of an auxiliary address pulse greater than 60 V helped improve the luminous efficiency in the cross-shaped cell.

IV. Conclusion

This paper proposed a highly efficient cross-shaped cell structure to improve the luminous efficiency of an ac-PDP. The microdischarge characteristics of the proposed structure were examined in an all-green 6-in test panel with various pressures and Xe-concentrations. Since the proposed cross-shaped cell structure has a longer ITO path between the two sustain electrodes and wider sidewall phosphor area, the following microdischarge characteristics were observed when compared with the conventional stripe-type cell structure.

1) The sustain voltage margin was lower by about 15 V under a high Xe-concentration of 10%.
2) The rate of increase in the luminous efficiency, ΔL, was higher under a high pressure and high Xe-concentration: with an Xe-concentration of 7%, $\Delta L = 0.56$ lm/W for the cross-shaped cell and $\Delta L = 0.38$ lm/W for the conventional cell when increasing the pressure from 300 to 600 torr, plus with a pressure of 450 torr and sustain voltage of 180 V, $\Delta L = 0.43$ lm/W for the cross-shaped cell and $\Delta L = 0.35$ lm/W for the conventional cell when increasing the Xe-concentration from 4 to 10%.
3) When adopting an auxiliary address pulse driving scheme, the luminous efficiency improved by about 44% (2.38 lm/W) with a high Xe-concentration of 10%.

References

[1] Y. Hashimoto, Y. Seo, O. Toyoda, K. Betsui, T. Kosaka, and F. Namiki, "High-luminance and highly luminous-efficient AC-PDP with DELTA cell structure," in *SID Dig.*, 2001, pp. 1328–1331.
[2] C. K. Yoon, J. K. Ahn, Y. J. Kim, S. H. Yoo, B. H. Lee, and K. S. Lee, "Optimization of delta color array for high-definition PDP with high-efficient hexagonal array structure," in *SID Dig.*, 2003, pp. 140–143.
[3] C. K. Yoon, J. H. Yang, W. J. Cheong, K. C. Choi, and K. W. Whang, "High luminance and efficiency AC-PDP with segmented electrode in delta color arrayed rectangular subpixels," in *IDW Dig.*, 2000, pp. 627–630.
[4] T. Yoshioka, A. Miyakoshi, A. Okigawa, E. Mizobata, and K. Toki, "A high luminance and high luminous efficiency AC-PDP using high Xe-content gas mixtures," in *IDW Dig.*, 2000, pp. 611–614.
[5] S.-H. Jang, K.-D. Cho, H.-S. Tae, K.-C. Choi, and S.-H. Lee, "Improvement of luminance and luminous efficiency using address voltage pulse during sustain-period of AC-PDP," *IEEE Trans. Electron Devices*, vol. 48, no. 9, pp. 1903–0910, Sep., 2002.
[6] K.-D. Cho, H.-S. Tae, and S.-I. Chien, "Improvement of color temperature using independent control of red, green, blue luminance in AC plasma display panel," *IEEE Trans. Electron Devices*, vol. 50, no. 2, pp. 359–365, Feb., 2003.
[7] J. C. Ahn, Y. Shintani, H. Tachibana, T. Sakai, and N. Kosugi, "Effects of pulsed potential on address electrode in a surface-discharge alternating-current plasma display panel," *Appl. Phys. Lett.*, vol. 82, no. 22, pp. 3844–3846, 2003.
[8] T. Nishio and K. Amemiya, "High-luminance and high definition 50-in. diagonal co-planar color PDPs with T-shaped electrodes," in *SID Dig.*, 1999, pp. 268–271.

Bo-Sung Kim received the M.S. degrees in electronic and electrical engineering in 2003 from Kyungpook National University, Daegu, Korea, where he is currently working toward the Ph.D. degree in electronic engineering.

His current research interests include plasma physics and high efficient novel structure in plasma display panels (PDPs).

Ki-Duck Cho received the B.S. degree from the School of Electrical Engineering and Computer Science and the M.S. and Ph.D. degrees in electronic engineering from Kyungpook National University Daegu, Korea, in 1999, 2001, and 2004, respectively.

Since 2003, he has been as senior research engineer at PDP Research Laboratory, LG Electronics, Gumi, Korea. His research interests include the driving circuit and driving waveform of plasma display panel.

Heung-Sik Tae (M'00) received the B.S. degree in electrical engineering and the M.S. and Ph.D. degrees in plasma engineering from Seoul National University, Seoul, Korea in 1986, 1988, and 1994, respectively.

Since 1995, he has been an Associate Professor at Kyungpook National University, Daegu, Korea. His research interests include the optical characterization and driving circuit of plasma display panels (PDPs), the design of millimeter wave guiding structures, and MEMS or thick-film processing for millimeter wave devices.

Dr. Tae is a Member of the Society for Information Display (SID). He has been serving as an Editor for the IEEE TRANSACTION on ELECTRON DEVICES section on flat panel display since 2005.

Sang-Hun Jang received the B.S. and M.S. degrees in electrical engineering and the Ph.D. degree in electronic engineering from Kyungpook National University, Daegu, Korea, in 1996, 1998, and 2002, respectively.

Since 2003, he has been a Member of the Research Staff of Samsung Advanced Institute of Technology, Suwon, Korea. His current research area is plasma display, especially development of highly efficient PDP.

Young-Mo Kim received the B.E. and M.E. degrees in nuclear engineering from Seoul National University, Seoul, Korea, in 1991 and 1993, respectively, and the Ph.D. degree in mechanical engineering from the Aachen University of Technology (RWTH), Aachen, Germany, in 1999.

From 1994 to 1999, he was a Guest Scientist at the Institute of Plasma Physics of Research Center, Juelich, Germany, working mainly on experimental plasma physics at a great fusion project (TEXTOR). Since 1999, he has been a Member of the Research Staff of Samsung Advanced Institute of Technology, Suwon, Korea. His current research area is plasma display, especially development of highly efficient PDP with new gas discharges.